PERGAMON

International Journal of Solids and Structures 36 (1999) 4183–4202

INTERNATIONAL JOURNAL OF SOLIDS and STRUCTURES

Interacting multiple cracks in piezoelectric materials

Xueli Han*, Tzuchiang Wang

LNM, Institute of Mechanics, Chinese Academy of Sciences, Beijing 100080, P.R. China

Received 12 March 1998; in revised form 2 June 1998

Abstract

In this paper, a method is presented to calculate the plane electro–elastic fields in piezoelectric materials with multiple cracks. The cracks may be distributed randomly in locations, orientations and sizes. In the method, each crack is treated as a continuous distributed dislocations with the density function to be determined according to the conditions of external loads and crack surfaces. Some numerical examples are given to show the interacting effect among multiple cracks.

1. Introduction

It is well known that piezoelectric materials produce an electric field when deformed, and undergo deformation when subjected to an electric field. The coupling nature of piezoelectric materials has attracted wide applications in electric–mechanical and electric devices, such as electric–mechanical actuators, sensors and transducers. In addition, they play an important role in the emerging technologies of smart materials and structures. When subjected to mechanical and electrical loads in service, these piezoelectric materials can fail prematurely due to their brittleness and presence of defects or flaws produced during their manufacturing process. Therefore, it is important to study the electro–elastic interaction and fracture behaviors of piezoelectric materials.

Although many studies have been made on the electro–elastic fracture mechanics based on the modeling and analysing of one crack in the piezoelectric materials (see, for example, Deeg, 1980; Pak, 1990, 1992; Sosa, 1992; Suo et al., 1992; Park and Sun, 1995a, b; Zhang and Tong, 1996; Zhang et al., 1998; Gao et al., 1997). To our knowledge, no efforts have been made to analyse the interacting fields among multiple cracks in these materials. In fact, piezoelectric materials (especially piezoceramics) are usually brittle and contain many cracks. The existence and interactions among these defects may greatly affect the material properties, especially the fracture behavior of these materials, which is sensitive to local electro–elastic fields.

This paper attempts to analyse the fracture behavior of interacting multiple cracks in piezoelectric

* Corresponding author. E-mail: hanxl@cc5.imech.ac.cn

PII: S0020–7683(98)00187–5

materials. It takes into consideration the locations, orientations and geometries of multiple cracks and analyses the electric–elastic fields. The method presented here is limited to two-dimensional problems. In the present analysis, each crack is described by a continuous distributed dislocations which includes electric-potential dislocations. The dislocation density function is expressed as a first Chebyshev polynomial series with a set of unknown coefficients, and the electric–elastic field can be expanded as series. The governing equations for the multiple crack problem are developed based on the basis of superposition technique and boundary collocation method, which is shown to have high computative efficiency and accuracy.

2. Basic formulae for a single crack

In this section, the extended Stroh formalism for piezoelectric plane problems (Barnett and Lothe, 1975; Pak, 1992; Suo et al., 1992) will be used.

In the absence of free charges and body forces, the elastic and electric field equations can be written as:

$$\sigma_{ij,i} = 0, \quad D_{i,i} = 0 \tag{1}$$

$$\sigma_{ij} = C_{ijrs}\gamma_{rs} - e_{sji}E_s, \quad D_i = \varepsilon_{is}E_s + e_{irs}\gamma_{rs} \tag{2}$$

where α, γ, $\mathbf{D}$ and $\mathbf{E}$ are stress, strain, electric displacement (electric induction) and electric field, respectively. The elastic, piezoelectric and dielectric constants of the medium are represented by the fourth-, third- and second-order tensors C, e and ε, respectively.

If $\mathbf{u}$ is the elastic displacement vector and ϕ the electric potential, the infinitesimal strain γ and the electric field $\mathbf{E}$ are derived from gradients:

$$\gamma_{ij} = \frac{1}{2}(u_{i,j} + u_{j,i}), \quad E_i = -\phi_{,i} \tag{3}$$

Substituting into eqn (2) yields,

$$\sigma_{ij} = C_{ijrs}u_{r,s} + e_{sji}\phi_{,s}, \quad D_i = -\varepsilon_{is}\phi_{,s} + e_{irs}u_{r,s} \tag{4}$$

Inserting into eqn (1) yields,

$$(C_{ijrs}u_r + e_{sji}\phi)_{,si} = 0, \quad (-\varepsilon_{is}\phi + e_{irs}u_r)_{,si} = 0 \tag{5}$$

For two-dimensional problems, in which all the fields are dependent on x and y only, the general solution can be sought in the form:

$$\mathbf{U} = \{u_r, \phi\}^T = \mathbf{a}f(\zeta_1 x + \zeta_2 y) \tag{6}$$

where $\mathbf{a} = (a_1, a_2, a_3, a_4)^T$ and the superscript T denotes the transpose. Without loss of generality, one can always take $\zeta_1 = 1$, $\zeta_2 = p$.

The number p and the column $\mathbf{a}$ are determined by substituting eqn (6) into (5), which gives

$$(C_{\alpha jr\beta}a_r + e_{\alpha j\beta}\alpha_4)\zeta_\alpha\zeta_\beta = 0, \quad (-\varepsilon_{\alpha\beta}a_4 + e_{\alpha r\beta}a_r)\zeta_\alpha\zeta_\beta = 0 \tag{7}$$

where α, $\beta = 1$ or 2. This is an eigenvalue problem consisting of four equations, a nontrivial $\mathbf{a}$ exists if p is a root of the determinant polynomial.

Since the eigenvalue p cannot be purely real (Suo et al., 1992), four conjugate pairs of p can be arranged as:

$$p_{\alpha+4} = \bar{p}_\alpha, \quad \mathrm{Im}\,(p_\alpha) > 0, \quad \alpha = 1, 2, 3, 4 \tag{8}$$

The most general real solution can be written as a linear combination of four arbitrary functions:

$$\mathbf{U} = \{u_r, \phi\}^T = 2\,\mathrm{Re} \sum_{\alpha=1}^{4} \mathbf{a}_\alpha f_\alpha(z_\alpha) \tag{9}$$

where $\mathbf{a}_\alpha$ is p_α associated eigenvector, and $z_\alpha = x + p_\alpha y$.

Furthermore, the stress and the electric displacement obtained from eqns (4) and (9) are given by

$$\mathbf{t} = \{\sigma_{2j,}\, D_2\}^T = 2\,\mathrm{Re} \sum_{\alpha=1}^{4} \mathbf{b}_\alpha f'_\alpha(z_\alpha) \tag{10}$$

$$\mathbf{s} = \{\sigma_{1j,} D_2\}^T = -2\,\mathrm{Re} \sum_{\alpha=1}^{4} \mathbf{b}_\alpha p_\alpha f'_\alpha(z_\alpha) \tag{11}$$

where for a pair (p, $\mathbf{a}$), the associated $\mathbf{b}$ is

$$b_j = (C_{2jr\beta} a_r + e_{\beta j2} a_4)\zeta_\beta = 0, \quad b_4 = (-\varepsilon_{1\beta} a_4 + e_{2r\beta} a_r)\zeta_\beta = 0 \tag{12}$$

Equations (6)–(12) are valid for $\gamma_{33} = E_2 = 0$ (plane strain and complex shear). For the case of $\sigma_{33} = E_3 = 0$ (plane stress and complex shear), the following substitution has to be made

$$C'_{ijrs} = C_{ijrs} - C_{ij33} C_{33rs}/C_{3333}, \quad e'_{sji} = e_{sji} - C_{ij33} e_{s33}/C_{3333}, \quad \varepsilon'_{is} = \varepsilon_{is} + e_{i33} e_{s33}/C_{3333}. \tag{13}$$

For the sake of convenience, we write the general solutions in compact forms as:

$$\mathbf{U} = 2\,\mathrm{Re}\,\{\mathbf{Af}(z)\} = \mathbf{Af}(z) + \overline{\mathbf{Af}(z)} \tag{14}$$

$$\mathbf{t} = 2\,\mathrm{Re}\,\{\mathbf{Bf}'(z)\} = \mathbf{Bf}'(z) + \overline{\mathbf{Bf}'(z)} \tag{15}$$

$$\mathbf{s} = -2\,\mathrm{Re}\,\{\mathbf{BPf}'(z)\} = -\mathbf{BPf}'(z) + \overline{\mathbf{BPf}'(z)} \tag{16}$$

where $\mathbf{A} = \{\mathbf{a}_1, \mathbf{a}_2, \mathbf{a}_3, \mathbf{a}_4\}$, $\mathbf{B} = \{\mathbf{b}_1, \mathbf{b}_2, \mathbf{b}_3, \mathbf{b}_4\}$, $\mathbf{P} = \mathrm{diag}\,\{p_1, p_2, p_3, p_4\}$, and $\mathbf{f}(z) = \{f_1(z_1), f_2(z_2), \mathbf{f}_3(\mathbf{z}_3), \mathbf{f}_4(\mathbf{z}_4)\}^T$.

Assuming there is a jump (called dislocation) in mechanical displacement as well as in electric potential at a point x of the $y = 0$ axis, define the jump as:

$$\mathbf{d}(x) = \mathbf{U}(x)^+ - \mathbf{U}(x)^- \tag{17}$$

Substituting into eqn (14), it can be expressed as

$$\mathbf{d}(x) = [\mathbf{Af}(x) - \overline{\mathbf{A}}\overline{\mathbf{f}}(x)]^+ - [\mathbf{Af}(x) - \overline{\mathbf{A}}\overline{\mathbf{f}}(x)]^- \tag{18}$$

For there is no electro-mechanical line loads in the solid $\mathbf{t}(x)$ is continuous across the x-axis, that is

$$\mathbf{t}(x)^{+} = \mathbf{t}(x)^{-} \tag{19}$$

From eqn (15) we have

$$[\mathbf{B}\mathbf{f}'(x) - \overline{\mathbf{B}\mathbf{f}}'(x)]^{+} = [\mathbf{B}\mathbf{f}'(x) - \overline{\mathbf{B}\mathbf{f}}'(x)]^{-} \tag{20}$$

So the function $\mathbf{B}\mathbf{f}'(z) - \overline{\mathbf{B}\mathbf{f}}'(z)$ can be analytically continued into the entire plane. Assuming there is no far field, the function must vanish on the whole plane, that is

$$\mathbf{B}\mathbf{f}'(z) = \overline{\mathbf{B}\mathbf{f}}'(z) \tag{21}$$

From eqns (18) and (21) we obtain

$$i\mathbf{d}'(x) = \mathbf{H}[\mathbf{h}^{+}(x) - \mathbf{h}^{-}(x)] \tag{22}$$

where

$$\mathbf{H} = \mathbf{Y} + \bar{\mathbf{Y}}, \quad \mathbf{Y} = i\mathbf{A}\mathbf{B}^{-1}, \quad \mathbf{h}(z) = \mathbf{B}\mathbf{f}'(z) \tag{23}$$

A crack in a piezoelectric solid can be represented by continuous distributed jump or dislocations (Pak, 1992). For a single crack of length $2a$ that lies on the $y = 0$ axis with the crack center at the coordinate origin, we can integrate the dislocation result (22) to obtain the total contribution of the distributed dislocations, as

$$\mathbf{H}\mathbf{h}(z) = \frac{1}{2\pi i}\int_{-a}^{a} \frac{i\mathbf{d}'(x)}{x - z}\,\mathrm{d}x \tag{24}$$

Considering the singular behavior of the dislocation density function, and noting the condition of the net dislocations of the crack being zero, we express $\mathbf{d}'(x)$ as the following series:

$$\mathbf{d}'(x) = -2\sum_{1}^{\infty} \mathbf{g}_m (1 - \tau^2)^{-1/2} T_m(\tau) \tag{25}$$

where $\tau = x/a$, $T_m()$ is Chebyshev polynomials of the first kind and $\mathbf{g}_m$ is vector to be determined.

Using the formula

$$\frac{1}{\pi}\int_{-1}^{1} \frac{(1-\tau^2)^{-1/2} T_m(\tau)}{z - \tau}\,\mathrm{d}\tau = R_m(z) \tag{26}$$

where $R_m(z) = (z - \sqrt{z^2 - 1})^m / \sqrt{z^2 - 1}$, from eqn (24), we obtain

$$\mathbf{H}\mathbf{h}(z) = \sum_{m=1}^{\infty} \mathbf{g}_m R_m(z/a) \tag{27}$$

Noting eqn (23), we have

$$\mathbf{f}'(z) = \mathbf{B}^{-1}\mathbf{H}^{-1} \sum_{m=1}^{\infty} \mathbf{g}_m \mathbf{R}_m(z/a) \tag{28}$$

Substituting the expression (28) for $\mathbf{f}'(z)$ into eqns (14)–(16), the electro–elastic fields can be expressed as series. Especially the quantity $\mathbf{t}(x)$ on the crack surface can be expressed as,

$$\mathbf{t}(x) = \mathbf{h}^{+}(x)+\mathbf{h}^{-}(x) = -2\mathbf{H}^{-1}\sum_{m=1}^{\infty}\mathbf{g}_m U_{m-1}(x/a) \tag{29}$$

where $U_{\mathrm{m}}()$ is Chebyshev polynomials of the second kind.

3. Multiple cracks in electroelastic media

This section concerns the problem of an electroelastic solid containing multiple nonintersecting cracks. Especially, consider an infinite plane containing some (such as N) arbitrarily oriented cracks, see Fig. 1, and the plane may be subjected to an arbitrary set of external electro–elastic loadings. Besides of a global Cartesian coordinate system Oxy, a set of local Cartesian systems $O_k x_k y_k$ ($k = 1, 2, \ldots, N$) situated at the center of each crack is employed with x_{k}-axis coincident with the crack surface. The k-th crack centers situates at C_{k}, the crack length is $2a_k$, and the crack surface makes angle θ_k with the Ox-axis.

On the crack surfaces, there is no traction or charge. Neglecting the electric induction in the environment, the electrical boundary condition along each crack surface is that the normal induction component should be zero, as proposed by Deeg (1980) and Pak (1990).

The problem of multiple interacting cracks in an electroelastic medium, as in an elastic medium, cannot be solved analytically except in special cases. As in solving the multiple interacting crack problems in an elastic medium, the superposition technique is often used, we also use it in present. The problem of multiple cracks in an electroelastic medium (which will be called the original problem) can be superimposed as a homogeneous problem and a perturbed problem. The homogeneous problem deals with the infinitely extended body without any cracks, subjected to the same external electro–elastic loading as the original problem. The perturbed problem is concerned with N cracks subject to no external loading. The perturbed problem is subdivided into N subproblems, each having only a single crack in an infinite body, subject to zero remote loading. Each single crack is modeled as an unknown distribution of dislocations along the crack line. The unknown

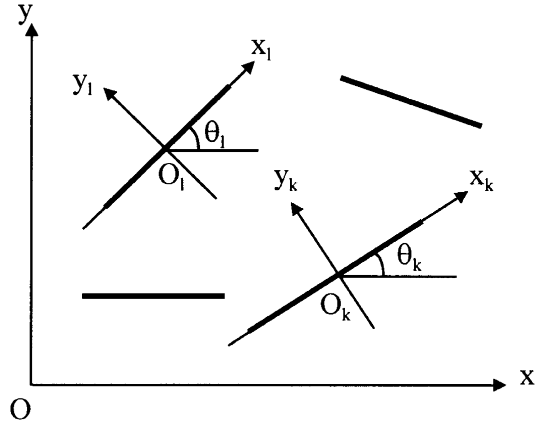

Fig. 1. An infinite plane with multiple cracks.

distribution of dislocations in each crack will need to be determined in such a way that all conditions for the original problem are satisfied.

Based on the superposition approach discussed above, the solution of a single crack in an infinitely extended electroelastic solid subject to an arbitrary jump in mechanical displacement and electric potential on the crack line (or distributed dislocations) is needed, and have been given out in the former section. These formulae are expressed in a system corresponding to the local coordinate one. The field $(\mathbf{t}^{(k)}, \mathbf{s}^{(k)})$ produced by the single k-th crack in the local coordinate system $O_k x_k y_k$ takes the form

$$\mathbf{t}^{(k)}(z^{(k)}) = 2\,\mathrm{Re}\,\{\mathbf{B}^{(k)}\mathbf{f}^{(k)\prime}(z^{(k)})\} \tag{30}$$

$$s^{(k)}(z^{(k)}) = -2\,\mathrm{Re}\,\{\mathbf{B}^{(k)}\mathbf{P}^{(k)}\mathbf{f}^{(k)\prime}(z^{(k)})\} \tag{31}$$

where the superscript (k) means quantities in the k-th local system.

From eqn (28), $\mathbf{f}^{(k)\prime}(z^{(k)})$ can be expressed as series in the local system, as

$$\mathbf{f}^{(k)\prime}(z^{(k)}) = \mathbf{B}^{(k)-1}\mathbf{H}^{(k)-1}\sum_{m=1}^{\infty}\mathbf{g}_m^{(k)}\mathbf{R}_m(z^{(k)}/a_k) \tag{32}$$

Then the field $(\mathbf{t}^{(k)}, \mathbf{s}^{(k)})$ can be expressed as series in any point. Especially, from eqn (29), the quantity $\mathbf{t}^{(k)}(x^{(k)})$ on the k-th crack surface can be expressed as series,

$$\mathbf{t}^{(k)}(x^{(k)}) = -2\mathbf{H}^{(k)-1}\sum_{m=1}^{\infty}\mathbf{g}_m^{(k)}U_{m-1}(x^{(k)}/a_k) \tag{33}$$

When the quantities $\mathbf{B}$, $\mathbf{P}$ and $\mathbf{H}$ in one coordinate system are calculated out, the corresponding quantities in the local system can be obtained by the transformation (Suo et al., 1992),

$$\mathbf{B}^{(k)} = \mathbf{RB}, \quad \mathbf{H}^{(k)} = \mathbf{RHR}^T, \quad p_j^{(k)} = (p_j\cos\theta - \sin\theta)/(p_j\sin\theta + \cos\theta) \tag{34}$$

where the transformation matrix $\mathbf{R}$ is

$$\mathbf{R} = \begin{bmatrix} \cos\theta & \sin\theta & 0 & 0 \\ -\sin\theta & \cos\theta & 0 & 0 \\ 0 & 0 & 1 & 0 \\ 0 & 0 & 0 & 1 \end{bmatrix} \tag{35}$$

and θ is the rotation angle of the local coordinate system from one coordinate system, such as from the global system to the k-th local system, then $\theta = \theta_k$.

Due to the contribution of the k-th crack, the stresses and normal electric induction along the presumed location of the l-th crack, can be written out according to the formulae of coordinate system transformation, as

$$\mathbf{t}^{(lk)} = \cos\theta^{(lk)}\mathbf{Rt}^{(k)} - \sin\theta^{(lk)}\mathbf{Rs}^{(k)} \tag{36}$$

where $\theta = \theta^{(lk)}$ in the transformation matrix $\mathbf{R}$, and $\theta^{(lk)}$ is the angle from the local coordinate axis-x_k to axis-x_l.

When the infinitely extended body is subject to mechanical and electrical loadings at infinity, the stresses and normal electric induction along the presumed location of the l-th crack in the crack-free homogeneous plane, produced by the far-field loadings, can be written out, and represented as $\mathbf{t}^{(l0)}$.

Summing the effect of all cracks and far-field loadings on the l-th crack, and imposing the boundary conditions on the crack surface, we have

$$\sum_{k=0}^{N} [\mathbf{t}^{(lk)}] = 0, \quad l = 1, 2, \ldots, N \tag{37}$$

These are the governing equations for N cracks in an infinite electro–elastic plane.

4. Numerical solution procedure and fracture parameters

Generally, the governing eqns (37) are not easy to solve analytically. We will solve them numerically by a crack surface collocation method.

On the l-th crack surface, we select M_l collocation points x_{li}, such as

$$x_{li} = a_l \cos\left(\frac{i\pi}{M_l+1}\right), \quad i = 1, 2, \ldots, M_l, \quad l = 1, 2, \ldots, N$$

and by truncating the series of the dislocation density function at the M_l term, then eqns (37) are reduced to a system of algebraic equations.

After solving these equations, the density function, mechanical and electrical fields produced by any one crack are known. According to the superposition principle, the fields produced by the multiple cracks are obtained with the aid of the transformation formulae from the local coordinate systems into the global one.

The main interest of this paper is to investigate local behavior of cracks, such as (stress and electric displacement) intensity factors, and energy release rates of cracks.

The electro–elastic fields are singular at crack tips. At a distance r ahead of the l-th crack tips,

$$\mathbf{t}^{(l)}(r) = (2\pi r)^{-1/2}\mathbf{K}^{(l)} \tag{38}$$

where $\mathbf{K}^{(l)} = \{K_2^{(l)}, K_1^{(l)}, K_3^{(l)}, K_D^{(l)}\}^T$ is defined as the stress and electric displacement intensity factors of the l-th crack.

The intensity factors can be expressed further as

$$\mathbf{K}^{(l)} = \pm 2\sqrt{\pi a_l}\mathbf{H}^{(l)-1}\sum_m \mathbf{g}_m^{(l)} T_m(\pm 1), \quad l = 1, 2, \ldots, N \tag{39}$$

where the quantities with upper and lower signs refer to the right- and left-hand tips of cracks, respectively.

At a distance r ahead of the l-th crack tips, the jump $\mathbf{d}^{(l)}$ is

$$\mathbf{d}^{(l)}(r) = (2r/\pi)^{1/2}\mathbf{H}^{(l)}\mathbf{K}^{(l)} \tag{40}$$

Since, in general, the matrix $\mathbf{H}$ contains off-diagonal elements, a K_D field will give rise to crack opening, and a K_1 field give rise to voltage between the crack faces.

The energy release rate at one tip of the l-th crack and along the crack line, can be written as (Suo et al., 1992),

$$G^{(l)} = \frac{1}{2\Lambda}\int_0^{\Lambda} \mathbf{t}^{(l)T}(\Lambda - r)\mathbf{d}^{(l)}(r)\mathrm{d}r \tag{41}$$

where Λ is an arbitrary length. It can be expressed further as

$$G^{(l)} = \frac{1}{4}\mathbf{K}^{(l)T}\mathbf{H}^{(l)}\mathbf{K}^{(l)} \tag{42}$$

Since, the matrix $\mathbf{H}$ is indefinite and with a negative component H_{44} (Suo et al., 1992), the energy release rate is not positive definite and always negative in the absence of mechanical loads. It is reduced by the presence of definite mechanical loads and a strong electric loading; it even has negative values.

When the total energy release rate is used as a fracture criterion, it indicates that the electric field always impedes crack growth, which is in contradiction to the experimental evidence that a positive electric loading aids crack propagation, while a negative electric field impedes crack growth (Tobin and Pak, 1993; Park and Sun, 1995b). Park and Sun (1995a, b) discussed the suitability of possible fracture criteria for piezoelectric materials, namely, the stress intensity factors, the total energy release rate and the mechanical energy release rate. They found that it may be more suitable to consider the mechanical energy release rate criterion as the fracture criterion, and this criterion predicts fracture loads accurately (Park and Sun, 1995b). The mechanical energy release rate for the l-th crack is

$$G^{M(l)} = \frac{1}{2\Lambda}\int_0^{\Lambda} \sigma_{i2}^{(l)T}(\Lambda - r)\Delta u_i^{(l)}(r)\mathrm{d}r \tag{43}$$

The fracture criterion for piezoelectric materials is still a debatable issue. About using the mechanical energy release rate as a fracture criterion, Park and Sun (1995a, b) argued that fracture is a mechanical process in nature and hence should be controlled only by the mechanical part of the energy. Though this argument seems not strict on physical grounds, the mechanical energy release rate criterion can well explain the experimental phenomena (Tobin and Pak, 1993; Park and Sun, 1995b). There may exist factors beyond the scope of linear piezoelectricity that would affect fracture behavior. A recent work by Gao et al. (1997) might shed some light on the fracture criterion. By analogy to the classical Dugdale model, Gao et al. (1997) proposed an electric strip saturation model, and derived the local energy release rate which gives linear prediction on electric field agreeing with the above-mentioned experimental results. Since it is assumed that the electric yielding zone remains unchanged during crack propagation, only the mechanical energy is taken into account in the local energy release rate. In this sense, the local energy release rate provides a physical basis to the mechanical energy release rate.

In the present paper, we adopt the mechanical release rate as the fracture criterion for the moment (the criterion will be discussed further later on), and focus attention on the interacting effects among cracks. For multiple cracks, besides the coupling behavior between elastic and electric fields, there are interacting effects among cracks. The interacting electroelastic fields of multiple cracks are very complex, their effects to fracture parameters of cracks should be analysed concretely.

5. Special case of practical significance

For a class of materials of practical significance: the poled ceramics, which has transverse symmetry around the poling axis (axis-3), its constitutive equation is given explicitly in Appendix A.

For a two-dimensional problem in which the (x, y)-plane coincides with the isotropic $(1, 2)$-plane, the in-plane deformation (u_x, u_y) is decoupled from the field (u_z, ϕ). The former is identical with the isotropic elasticity problem. The latter can be simplified greatly, as only u_z and ϕ exist.

The more practical case on which we will focus, is when the two-dimensional (x, y)-plane coincides with the isotropic $(1, 3)$-plane. For this case, the characteristic equation becomes,

$$\begin{bmatrix} c_{11}+c_{44}p^2 & (c_{13}+c_{44})p & 0 & (e_{31}+e_{15})p \\ (c_{13}+c_{44})p & c_{44}+c_{33}p^2 & 0 & e_{15}+e_{33}p^2 \\ 0 & 0 & (c_{11}-c_{12})/2+c_{44}p^2 & 0 \\ (e_{31}+e_{15})p & e_{15}+e_{33}p^2 & 0 & -\varepsilon_{11}-\varepsilon_{33}p^2 \end{bmatrix} \begin{bmatrix} a_1 \\ a_2 \\ a_3 \\ a_4 \end{bmatrix} = 0 \tag{44}$$

The determinant equation of the eigenvalue problem is,

$$(c_{11}-c_{12}+2c_{44}p^2)(c_0p^6+c_1p^4+c_2p^2+c_3) = 0 \tag{45}$$

with

$$\begin{aligned} c_0 &= c_{44}e_{33}^2+c_{33}c_{44}\varepsilon_{33} \\ c_1 &= c_{33}(e_{31}+e_{15})^2-2c_{13}e_{33}(e_{31}+e_{15})+c_{11}e_{33}^2-2c_{44}e_{31}e_{33}+c_{33}c_{44}\varepsilon_{11} \\ &\quad +(c_{11}c_{33}-c_{13}^2-2c_{13}c_{44})\varepsilon_{33} \\ c_2 &= 2c_{11}e_{13}e_{33}-2c_{13}e_{15}(e_{15}+e_{31})+c_{44}e_{31}^2+(c_{11}e_{33}-c_{13}^2-2c_{13}c_{44})\varepsilon_{11}+c_{11}c_{44}\varepsilon_{33} \\ c_3 &= c_{11}e_{15}^2+c_{11}c_{44}\varepsilon_{11} \end{aligned}$$

For a pair $(p, \mathbf{a})$, the associated $\mathbf{b}$ is

$$\begin{bmatrix} b_1 \\ b_2 \\ b_3 \\ b_4 \end{bmatrix} = \begin{bmatrix} c_{44}p & c_{44} & 0 & e_{15} \\ c_{13} & c_{33}p & 0 & e_{33}p \\ 0 & 0 & c_{44}p & 0 \\ e_{31} & e_{33}p & 0 & -\varepsilon_{33}p \end{bmatrix} \begin{bmatrix} a_1 \\ a_2 \\ a_3 \\ a_4 \end{bmatrix} \tag{46}$$

Equations (44)–(46) are valid for plane strain and complex shear deformation $(\gamma_{zz} = E_z = 0)$. Assuming $\sigma_{zz} = E_z = 0$, the plane stress and complex shear problem can be treated by a change of material constants as,

$$C'_{11}=C_{11}-\frac{C_{12}^2}{C_{11}},\quad C'_{12}=C_{12}-\frac{C_{12}^2}{C_{11}},\quad C'_{13}=C_{13}-\frac{C_{12}C_{13}}{C_{11}},\quad C'_{33}=C_{33}-\frac{C_{13}^2}{C_{11}}$$

$$e'_{31}=\left(1-\frac{C_{12}}{C_{11}}\right)e_{31},\quad e'_{33}=e_{33}-\frac{C_{13}}{C_{11}}e_{31},\quad \varepsilon'_{33}=\varepsilon_{33}+\frac{e_{31}^2}{C_{11}} \tag{47}$$

Solving the eigenvalue problem, the characteristic roots and associated vectors are known. Especially, the matrix **H** has a structure as

$$\mathbf{H}=\begin{bmatrix} \frac{2}{C_L} & 0 & 0 & 0 \\ 0 & \frac{2}{C_T} & 0 & \frac{2}{e} \\ 0 & 0 & \frac{2}{C_A} & 0 \\ 0 & \frac{2}{e} & 0 & -\frac{2}{\varepsilon} \end{bmatrix} \tag{48}$$

6. Numerical examples and discussion

We first consider a material that the piezoelectric tensor vanishes, then the elastic field is decoupled from the electric one. For this case, the elastic fields of interacting multiple cracks calculated by the present method conform to the corresponding results in an elastic plane. An example is given to show the accuracy and efficiency of the present method. Consider two equal collinear cracks in an infinite isotropic plane under a remote uniform tension as seen in Fig. 2. With the piezoelectric tensor vanishes and the elasticity tensor tends to isotropic one, the normalized

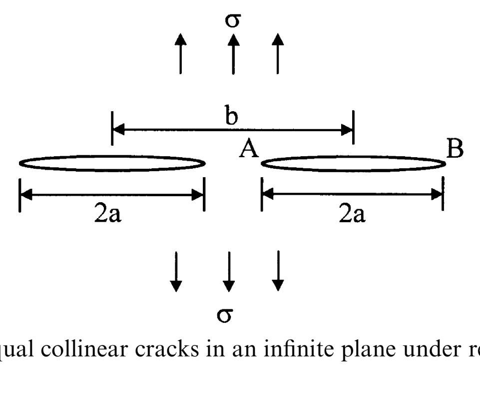

Fig. 2. Two equal collinear cracks in an infinite plane under remote tension.

Table 1
The normalized SIF $k(=K/\sigma\sqrt{\pi a})$ for two equal collinear cracks in an infinite isotropic plane under remote tension

		k at tip A		k at tip B	
$2a/b$	M	Present	Exact	Present	Exact
0.10	3	1.00132	1.00132	1.00120	1.00120
0.20	4	1.00566	1.00566	1.00462	1.00462
0.30	4	1.01383	1.01383	1.01017	1.01017
0.40	5	1.02717	1.02717	1.01787	1.01787
0.50	6	1.04796	1.04796	1.02795	1.02795
0.60	7	1.08040	1.08040	1.04094	1.04094
0.70	9	1.13326	1.13326	1.05786	1.05786
0.80	14	1.22894	1.22894	1.08107	1.08107
0.90	18	1.45387	1.45387	1.11741	1.11741

stress intensity factors obtained by the present method are shown in Table 1. The series terms M needed to get them are listed also. From the table we can see that the results converge to the exact solutions of Erdogan (1962) with high accuracy. Though the number M of series terms needed is high, to assure a result with so high accuracy (with six figures accuracy here), when the crack distance is very small, but in reality, only few terms of series are enough to give out quite accurate results.

In this section, we can take an example material such as PZT-5H ceramic as the piezoelectric medium. The poled PZT-5H ceramic exhibits transversely isotropic behavior with the axis-3 as the poling direction, and the material properties are given in Appendix B. Among many possible crack orientations, we will focus on a particular orientation, that is the (x, y)-plane which containing cracks coincides with the material anisotropic $(1, 3)$-plane, see Fig. 3.

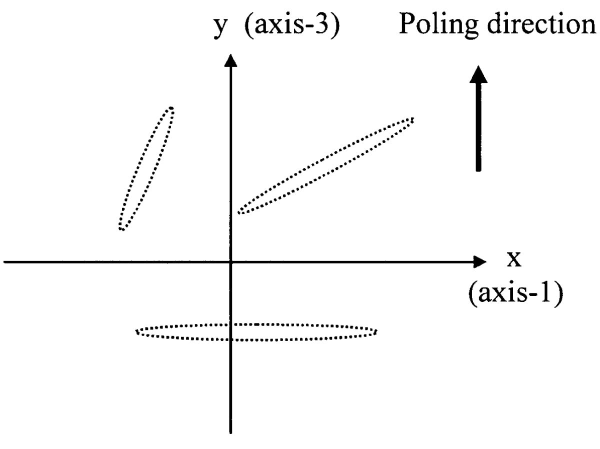

Fig. 3. Alignment of the coordinate system with principal material axis.

For a single crack of length a along the x-axis and the plane under far-field loads, the intensity factors calculated by the present method are the exact ones,

$$\{K_2, K_1, K_3, K_D\} = \{\sqrt{\pi a}\sigma_{yx}^{\infty}, \sqrt{\pi a}\sigma_{y}^{\infty}, \sqrt{\pi a}\sigma_{yz}^{\infty}, \sqrt{\pi a}D_{y}^{\infty}\}$$

This simple result holds for any kind of piezoelectric materials with arbitrary anisotropic orientation.

For this case, the matrix $\mathbf{H}$ has the structure of eqn (48). For plane strain and complex shear, we have

$$\frac{2}{C_L} = 3.51034\times10^{-11}, \quad \frac{2}{C_T} = 3.21311\times10^{-11}, \quad \frac{2}{C_A} = 5.64974\times10^{-11}\frac{m^2}{N},$$

$$\frac{2}{\varepsilon} = 9.15587\times10^{7}\frac{Vm}{C}, \quad \frac{2}{e} = 2.55506\times10^{-2}\frac{m^2}{C}.$$

While for plane stress and complex shear case,

$$\frac{2}{C_L} = 4.10930\times10^{-11}, \quad \frac{2}{C_T} = 3.49723\times10^{-11}, \quad \frac{2}{C_A} = 5.64974\times10^{-11}\frac{m^2}{N},$$

$$\frac{2}{\varepsilon} = 8.83426\times10^{7}\frac{Vm}{C}, \quad \frac{2}{e} = 2.85439\times10^{-2}\frac{m^2}{C}$$

which have higher values than for plane strain and complex shear case. In following numerical examples, we focus on plane strain case. The total energy release rate for the single crack is,

$$G = \frac{\pi a}{2}\left(\frac{1}{C_L}\sigma_{yx}^{\infty 2} + \frac{1}{C_T}\sigma_{y}^{\infty 2} + \frac{1}{C_A}\sigma_{yz}^{\infty 2} + \frac{2}{e}\sigma_{y}^{\infty} D_{y}^{\infty} - \frac{1}{\varepsilon}D_{y}^{\infty 2}\right).$$

For plane strain and complex shear case, G has the same value for PZT-5H as that given by Pak (1992). When G is used as a fracture criterion, it indicates that the electric field always impedes crack growth for which there is no experimental support.

Park and Sun (1995a, b) found that the mechanical energy release rate criterion is superior to other fracture criteria and predicts fracture loads fairly accurately (1995b). The mechanical energy release rate for the single crack is,

$$G^{M} = \frac{\pi a}{2}\left(\frac{1}{C_L}\sigma_{yx}^{\infty 2} + \frac{1}{C_T}\sigma_{y}^{\infty 2} + \frac{1}{C_A}\sigma_{yz}^{\infty 2} + \frac{1}{e}\sigma_{y}^{\infty} D_{y}^{\infty}\right)$$

The dependence of the mode I mechanical energy release rate G_{I}^{M} on D_{y}^{∞} is linear. A positive electric loading increases it and a negative electric loading decreases it, while the electric loading has no influence to the mode II and mode III ones. A pure electric loading cannot induce mechanical energy release rate.

Considering an electrical yielding condition, the local energy release rate may be a promising candidate for fracture criteria. The local energy release rate for the single electrically yielded crack is (Gao et al., 1997; Wang, 1998),

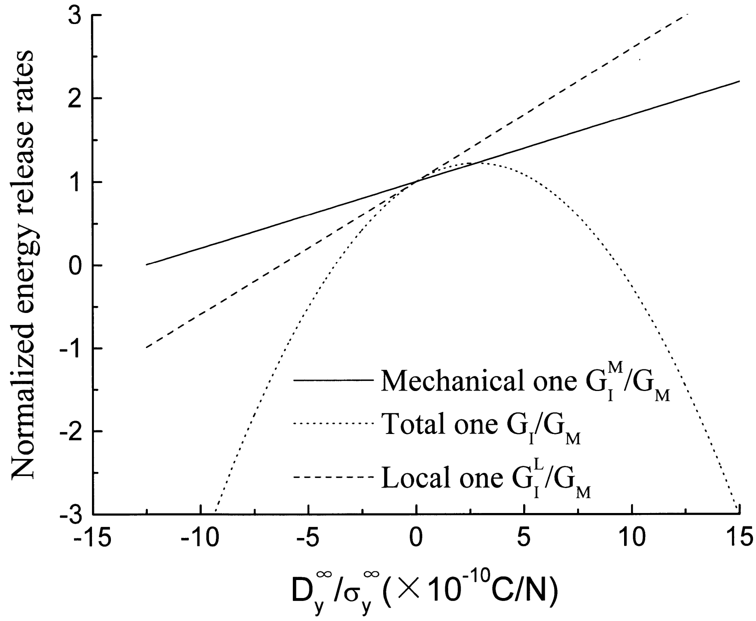

Fig. 4. The energy release rates for a single crack as a function of $D_y^\infty/\sigma_y^\infty$.

$$G^L = \frac{\pi a}{2}\left(\frac{1}{C_L}\sigma_{yx}^{\infty 2} + \frac{1}{C_T}\sigma_y^{\infty 2} + \frac{1}{C_A}\sigma_{yz}^{\infty 2} + \frac{2}{e}\sigma_y^\infty D_y^\infty + \frac{C_T}{e^2}D_y^{\infty 2}\right)$$

As for the mechanical energy release rate, the local mode I energy release rate is increased by a positive electric loading, and decreased by a negative one. The local energy release rate due to mode II and mode III mechanical loading has no coupling effect with that due to electric loading. A pure positive electric loading D_y^∞ induces a local energy release rate $\pi a/2C_T/e^2 D_y^{\infty 2}$, a negative one induces crack closing, while D_x^∞ has no influence to energy release rate (both total and local ones), this result may provide a possible explanation of the experimental phenomena: cyclic electric field perpendicular to a crack can induce fatigue crack growth, while a parallel one has no influence (Cao and Evans, 1994).

Figure 4 shows the normalized mode I mechanical energy release rate G_I^M/G_M, the local energy release rate G_I^L/G_M and the total energy release rate G_I/G_M for varying $D_y^\infty/\sigma_y^\infty$, where $G_M = \pi a/(2C_T)\,\sigma_y^{\infty 2}$ is the energy release rate without electric loading. For an applied tension loading and $D_y^\infty/\sigma_y^\infty > -e/C_T(= -1.26\times 10^{-9}\ C/N)$, G_I^M is positive and dependent linearly on D_y^∞, and the crack surface is opened. Similar as G_I^M, G_I^L is dependent roughly linearly on D_y^∞. Without mechanical loading, G_I^M is zero, while $G_I^L > 0$ for $D_y^\infty > 0$. On the other hand, $G_I < G_M$ when the electric load is outside the range $0 < D_y^\infty/\sigma_y^\infty < 2\varepsilon/e(= 0.558\times 10^{-9}\ C/N)$, and G_I becomes negative when outside the range $-0.376\times 10^{-9} < D_y^\infty/\sigma_y^\infty < 0.934\times 10^{-9}\ C/N$. Without mechanical loading, G_I is always negative.

For other anisotropic orientation, such as the y-axis make an angle θ with the poling axis-3, the matrix $\mathbf{H}$ in the (x, y) coordinate system can be obtained by a transformation. The mechanical energy release rate and local energy release rate respectively are,

$$G^M = \frac{\pi a}{2}\left[\left(\frac{c^2}{C_L}+\frac{s^2}{C_T}\right)\sigma_{yx}^{\infty 2}+\left(\frac{s^2}{C_L}+\frac{c^2}{C_T}\right)2]\sigma_y^{\infty 2}+2\left(-\frac{cs}{C_L}+\frac{cs}{C_T}\right)\sigma_y^{\infty}\,\sigma_{yx}^{\infty}\right.$$

$$\left.+\frac{1}{C_A}\sigma_{yz}^{\infty 2}+\frac{c}{e}\sigma_y^{\infty}\,D_y^{\infty}+\frac{s}{e}\sigma_{yx}^{\infty}\,D_y^{\infty}\right]$$

$$G^L = \frac{\pi a}{2}\left[\left(\frac{c^2}{C_L}+\frac{s^2}{C_T}\right)\sigma_{yx}^{\infty 2}+\left(\frac{s^2}{C_L}+\frac{c^2}{C_T}\right)\sigma_y^{\infty 2}+2\left(-\frac{cs}{C_L}+\frac{cs}{C_T}\right)\sigma_y^{\infty}\,\sigma_{yx}^{\infty}\right.$$

$$\left.+\frac{1}{C_A}\sigma_{yz}^{\infty 2}+2\frac{c}{e}\sigma_y^{\infty}\,D_y^{\infty}+2\frac{s}{e}\sigma_{yx}^{\infty}\,D_y^{\infty}+\frac{C_T}{e^2}D_y^{\infty 2}\right]$$

where c and s denote $\cos\theta$ and $\sin\theta$, respectively. It can be seen that, in this case the electric loading has no influence to G_{III}^M. For $\theta = 90^\circ$, that is the crack along the poling direction, G_{I}^M is independent on the electric loading, while G_{II}^M is dependent on it linearly. For other directions except crack along or perpendicular to the poling direction, G_{I}^M and G_{II}^M are dependent linearly on the electric loading. The influence of electric loading to G^L is similar as it to G^M, except pure electric loading contributes nothing to G^M but $\pi a/2C_T/e^2 D_y^{\infty 2}$ to G^L.

The fracture criterion based on total energy release rate has doubtful issue and difficulty in explaining experiments. Fracture criteria based on mechanical energy release rate and on local energy release rate can expect a similar effect of electric loading (except pure electric loading) and these criteria seem to be in broad agreement with experimental observations. For above-mentioned reasons, and considering our analysis is on the basis of linear electro–elasticity, in the following we will mainly use the mechanical energy release rate as a criterion to investigate its change due to crack interacting effect.

For two equal collinear cracks in piezoelectric materials as shown in Fig. 2, subjected to far plane loads, the normalized intensity factors at one tip have a same value k, that is, at one crack tip,

$$\frac{K_2}{\sqrt{\pi a}\sigma_{yx}^{\infty}} = \frac{K_1}{\sqrt{\pi a}\sigma_y^{\infty}} = \frac{K_D}{\sqrt{\pi \alpha}D_y^{\infty}} = k$$

and k is the same as the normalized stress intensity factors in Table 1 for isotropic materials. Thus the energy release rate G and the mechanical energy release rate G^M at one tip of collinear cracks are,

$$G = k^2 G_0, \quad G^M = k^2 G_0^M$$

where G_0 and G_0^M are the corresponding energy release rate and mechanical energy rate for a single crack without interaction with other cracks. These results hold for any collinear cracks in piezoelectric materials with arbitrary anisotropic orientation. Which means, if the fracture behavior of a single crack in some direction under some loadings is known, the interacting effect of collinear cracks is just like the effect in isotropic elastic materials.

Figure 5(a) shows three equal parallel cracks along x-axis in PZT-5H ceramic, subjected to far plane loads. For the central crack, the normalized intensity factors $k_2(=K_2/\sqrt{\pi\alpha}\sigma_{yx}^{\infty})$, $k_1(=K_1/\sqrt{\pi a}\sigma_y^{\infty})$ and $k_D(=K_D/\sqrt{\pi a}D_y^{\infty})$ against d/a are plotted in Fig. 5(b). From the figure we can see that, $k_1<1$ and $k_D<1$ for any d. The mechanical energy release rate for the central crack is

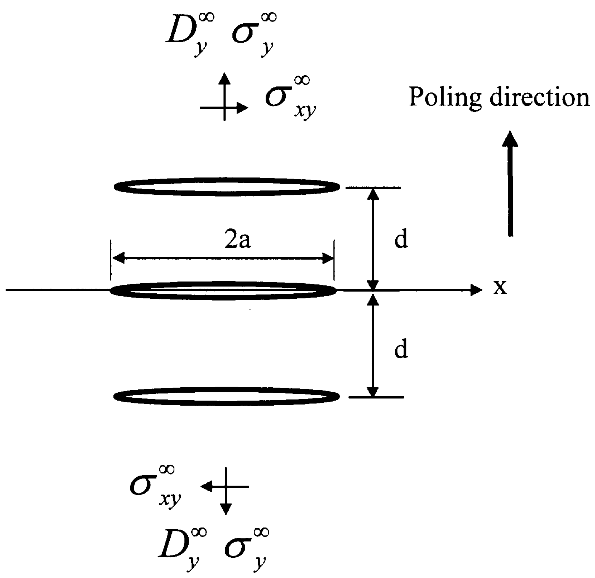

Fig. 5(a). Schematic of three equal parallel cracks.

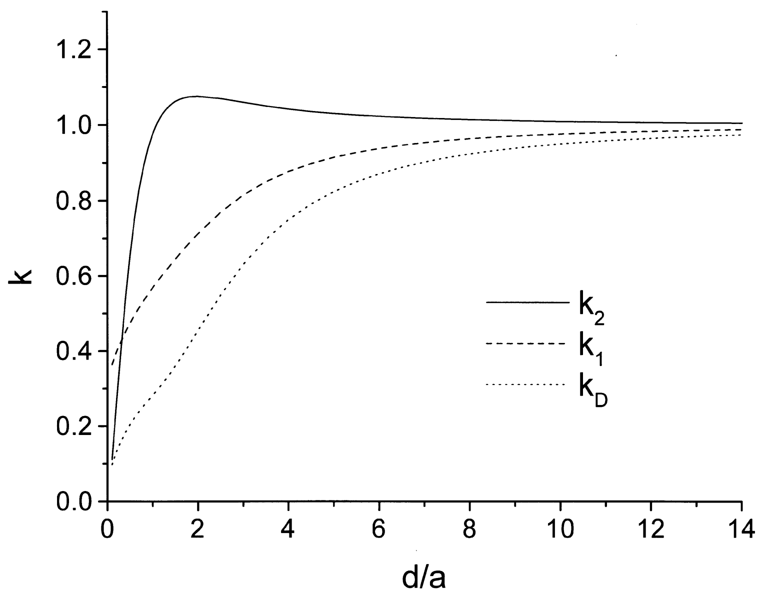

Fig. 5(b). The normalized intensity factors of the central crack against d/a.

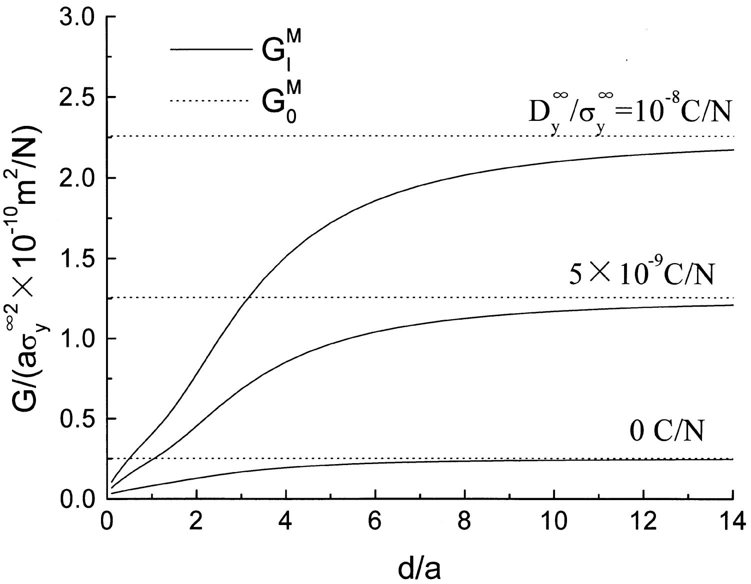

Fig. 5(c). The mode I mechanical energy release rate $G_{\rm I}^M$ of the central crack against d/a.

$$G^M = \frac{\pi a}{2}\left(k_2^2\frac{1}{C_L}\sigma_{yx}^{\infty 2}+k_1^2\frac{1}{C_T}\sigma_y^{\infty 2}+k_1k_D\frac{1}{e}\sigma_y^\infty D_y^\infty\right)$$

For mode II fracture, $G_{\rm II}^M$ is not dependent on the electric loading. For mode I fracture, $G_{\rm I}^M$ is plotted in Fig. 5(c) against d/a for different $D_y^\infty/\sigma_y^\infty$. The energy $G_{\rm I}^M$ is dependent linearly on D_y^∞, and always litter than the corresponding energy rate G_0^M for the crack without interaction with other cracks, and tends to it for $d/a\to\infty$. So, under mode I fracture, the stacked cracks can shield the fracture of the central crack.

Figure 6(a) shows a crack array in PZT-5H ceramic subjected to loads σ_y^∞ and D_y^∞, in which the center crack is perpendicular to the axis-3 and surrounded by four symmetrically distributed equal cracks. The normalized intensity factors and mechanical energy release rates of the central crack against the crack length ratio $2l/(b-a)$ are plotted in Fig. 6(b) and (c), respectively, with $(a+b)/l_0 = 4$, $(b-a)/l_0 = 0.5$, and $d/(b-a) = 0.8$, where $2l_0$ is the original length of the central crack. When the main crack is away from the surrounding cracks, $k_2 > 1$, $k_D > 1$, and $G_{\rm I}^M > G_0^M$, where G_0^M is the corresponding energy rate for the single crack without interaction with other cracks. This means the main crack is amplified. When the main crack is under the surrounding cracks, $k_2 < 1$, $k_D < 1$, and $G_{\rm I}^M < G_0^M$. This means the main crack is shielded. The amplification and shielding domain is similar as the crack array in an anisotropic material with the same elastic constants as those in the piezoelectric material.

Under pure electric loading, the mechanical energy release rate is zero. In this case, the interacting effect among cracks can be determined by the change of electric intensity factor. As the change of K_D almost always has a similar tendency as the change of K_1 due to crack interaction (K_D and K_1 are greater or less than one almost at the same time), which implies the interacting effect (shielding

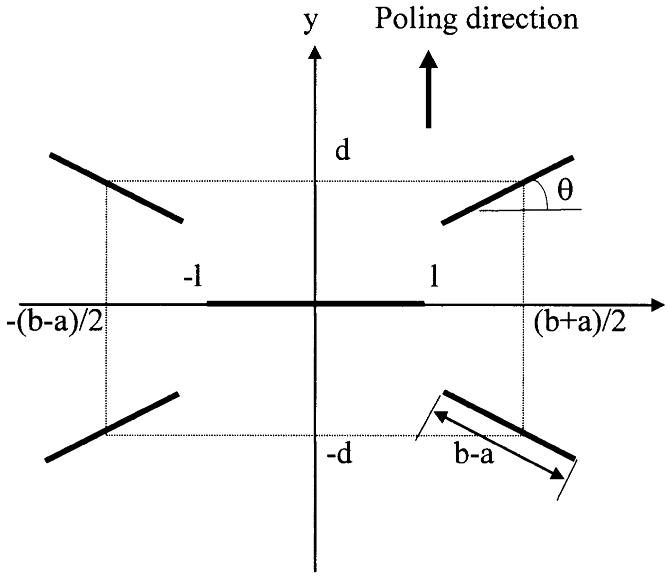

Fig. 6(a). Schematic of a central crack surrounded by four identical cracks.

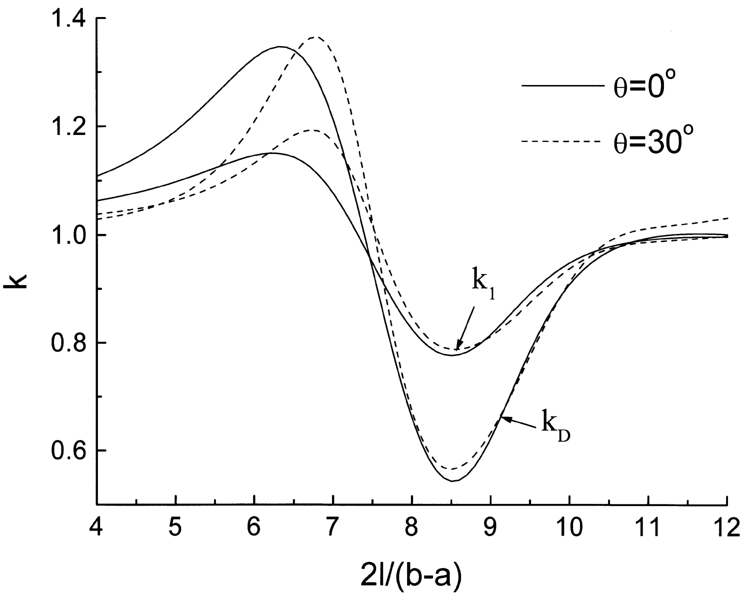

Fig. 6(b). The normalized intensity factors of the central crack against $2l/(b-a)$.

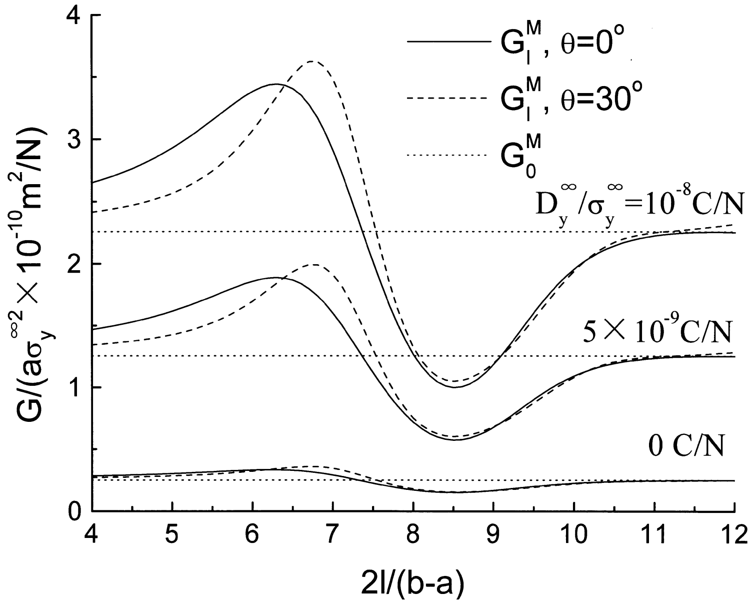

Fig. 6(c). The mode I mechanical energy release rate G_I^M of the central crack against $2l/(b-a)$.

or amplifying) among cracks under pure electric loading is just like it is under mode I mechanical loading.

7. Conclusions and remarks

A method is presented to calculate the elasto–electric fields of multiple cracks in piezoelectric materials. The interacting effects among cracks are investigated through some examples. As cracks in anisotropic materials, in general, if crack locations are biased towards stacked arrangements, then the shielding effect of interactions will dominate, on the other hand, amplifying effect will dominate.

Though the interacting effects among cracks are obtained through some examples on combined electric-mechanical loading conditions, the conclusions are also true for pure electric loading conditions. Under pure electric loading, though the mechanical energy release rate is zero, but the interacting effect among cracks can be determined by the change of electric intensity factor. As the change of K_D almost always has a similar tendency as the change of K_I due to crack interaction (K_D and K_I are greater or less than one almost at the same time), which implies the interacting effect (shielding or amplifying) among cracks under pure electric loading is just like it under mode I mechanical loading. The numerical examples are focused on plane strain deformation. For plane stress case, though the energy release rates are different from that for plane strain case (higher than that), but the interacting effects among cracks will be similar as that under plane strain deformation.

Acknowledgements

The authors are grateful for financial support by the National Natural Science Foundation of China (No. 19704100) and the Natural Science Foundation of Chinese Academy of Sciences (project KJ951-1-201). Support by the National Youth Natural Science Foundation of China (No. 19602020) is gratefully acknowledged by the first author.

Appendix A

Let axis-3 be poling direction of transversely isotropic piezoelectrics. The constitutive relations for the materials are given by

$$\begin{bmatrix}\sigma_{11}\\ \sigma_{22}\\ \sigma_{33}\\ \sigma_{23}\\ \sigma_{31}\\ \sigma_{12}\end{bmatrix} = \begin{bmatrix} c_{11} & c_{12} & c_{13} & 0 & 0 & 0\\ c_{12} & c_{11} & c_{13} & 0 & 0 & 0\\ c_{13} & c_{13} & c_{33} & 0 & 0 & 0\\ 0 & 0 & 0 & c_{44} & 0 & 0\\ 0 & 0 & 0 & 0 & c_{44} & 0\\ 0 & 0 & 0 & 0 & 0 & (c_{11}-c_{12})/2 \end{bmatrix} \begin{bmatrix}\gamma_{11}\\ \gamma_{22}\\ \gamma_{33}\\ 2\gamma_{23}\\ 2\gamma_{31}\\ 2\gamma_{12}\end{bmatrix} - \begin{bmatrix} 0 & 0 & e_{31}\\ 0 & 0 & e_{31}\\ 0 & 0 & e_{33}\\ 0 & e_{15} & 0\\ e_{15} & 0 & 0\\ 0 & 0 & 0\end{bmatrix} \begin{bmatrix}E_1\\ E_2\\ E_3\end{bmatrix}$$

$$\begin{bmatrix}D_1\\ D_2\\ D_3\end{bmatrix} = \begin{bmatrix} 0 & 0 & 0 & 0 & e_{15} & 0\\ 0 & 0 & 0 & e_{15} & 0 & 0\\ e_{31} & e_{31} & e_{33} & 0 & 0 & 0\end{bmatrix} \begin{bmatrix}\gamma_{11}\\ \gamma_{22}\\ \gamma_{33}\\ 2\gamma_{23}\\ 2\gamma_{31}\\ 2\gamma_{12}\end{bmatrix} + \begin{bmatrix}\varepsilon_{11} & 0 & 0\\ 0 & \varepsilon_{11} & 0\\ 0 & 0 & \varepsilon_{33}\end{bmatrix} \begin{bmatrix}E_1\\ E_2\\ E_3\end{bmatrix}$$

Appendix B

Material properties for PZT-5H (Pak, 1992):

$c_{11} = 126$ GPa,
$c_{12} = 55$ GPa,
$c_{13} = 53$ GPa,
$c_{33} = 117$ GPa,
$c_{44} = 35.3$ GPa,
$e_{31} = -6.5$ C/m^2,
$e_{33} = 23.3$ C/m^2,
$e_{15} = 17$ C/m^2,
$\varepsilon_{11} = 151 \times 10^{-10}$ C/Vm,
$\varepsilon_{33} = 130 \times 10^{-10}$ C/Vm.

References

Barnett, D.M., Lothe, J., 1975. Dislocations and line charges in anisotropic piezoelectric insulators. Phys. Stat. Sol. (b) 67, 105–111.

Cao, H.C., Evans, A.G., 1994. Electric-field-induced fatigue crack growth in piezoelectric ceramics. J. Am. Ceram. Soc. 77, 1783–1786.

Deeg, W.E.F., 1980. The analysis of dislocation, crack and inclusion problems in piezoelectric solids. Ph.D. thesis, Stanford University.

Erdogan, F., 1962. On the stress distribution in plates with collinear cuts under arbitrary loadings. Proc. 4th U.S. Nat. Congr. Appl. Mech., pp. 547–553.

Gao, H., Zhang, T.Y., Tong, P., 1997. Local and global energy rates for an electrically yielded crack in piezoelectric ceramics. J. Mech. Phys. Solids 45, 491–510.

Pak, Y.E. 1990. Crack extension force in a piezoelectric material. J. Appl. Mech. 57, 647–653.

Pak, Y.E. 1992. Linear electro–elastic fracture mechanics of piezoelectric materials. Int. J. Fracture 54, 79–100.

Park, S.B., Sun, C.T. 1995a. Effect of electric field on fracture of piezoelectric ceramics. Int. J. Fracture 70, 203–216.

Park, S.B., Sun, C.T., 1995b. Fracture criteria for piezoelectric ceramics. J. Am. Ceram. Soc. 78, 1475–1480.

Sosa, H., 1992. On the fracture mechanics of piezoelectric solids. Int. J. Solids Structures 29, 2613–2622.

Suo, Z., Kuo, C.-M., Barnett, D.M., Willis, J.R., 1992. Fracture mechanics for piezoelectric ceramics. J. Mech. Phys. Solids 40, 739–765.

Tobin, A.G., Pak, Y.E., 1993. Effects of electric field on fracture of piezoelectric ceramics. Proc. SPIE, Smart Struct. Mater. 1916, 78–86.

Wang, T.C., 1998. Analysis of strip electric saturation model of crack problem in piezoelectric materials. Int. J. Solids Structures, submitted.

Zhang, T.Y., Tong, P., 1996. Fracture mechanics for a mode III crack in a piezoelectric material. Int. J. Solids Structures 33, 343–359.

Zhang, T.Y., Qian, C.F., Tong, P, 1998. Linear electro–elastic analysis of a cavity or a crack in a piezoelectric material. Int. J. Solids Structures 35, 2121–2149.